

Influence of boundary conditions on quantum escape

ORESTIS GEORGIU¹, GORAN GLIGORIĆ^{1,2}, ACHILLEAS LAZARIDES¹, DIEGO F. M. OLIVEIRA^{1,3},
JOSHUA D. BODYFELT¹ and ARSENI GOUSSEV^{1,4}

¹ *Max Planck Institute for the Physics of Complex Systems - Nöthnitzer Straße 38, D-01187, Dresden, Germany, EU*

² *Vinča Institute of Nuclear Sciences, University of Belgrade - P.O. Box 522, 11001 Belgrade, Serbia*

³ *Institute for Multiscale Simulations, Friedrich-Alexander Universität - Naegelsbachstrasse 49b, D-91052, Erlangen, Germany, EU*

⁴ *School of Computing, Engineering and Information Sciences, Northumbria University Newcastle Upon Tyne, NE1 8ST, UK, EU*

received 23 July 2012; accepted in final form 1 October 2012
published online 31 October 2012

PACS 05.60.Gg – Quantum transport

PACS 03.65.Ge – Solutions of wave equations: bound states

PACS 71.10.-w – Theories and models of many-electron systems

Abstract – It has recently been established that quantum statistics can play a crucial role in quantum escape. Here we demonstrate that boundary conditions can be equally important—moreover, in certain cases, may lead to a complete suppression of the escape. Our results are exact and hold for arbitrarily many particles.

Copyright © EPLA, 2012

Introduction and setup. – The question of how particles escape from a partially confining region has long been at the center of many experimental and theoretical studies, leading to a number of profound discoveries in mathematical physics (for a recent review see ref. [1]). Most of the theoretical progress has been made in the context of classical mechanics, where different dynamical behaviors—regular, chaotic, or mixed—lead to different escape laws; typically quantified by the decay of the survival (*i.e.*, non-escape) probability. On the quantum-mechanical side, there has been a surge of renewed interest in the escape properties of few-particle systems [2–9], in connection with recent advances in experimental control and manipulation of a small number of ultra-cold atoms [10,11]. In particular, particle-particle interactions and quantum statistics have been shown to significantly influence the escape. Here, we extend the theory to account for the influence of boundary conditions and derive an exact quantum propagator which is valid for all times and for the most general case of homogeneous boundary conditions [12].

We consider a system of N non-interacting particles in one spatial dimension which are initially confined within the interval $I = (0, 1)$ with a hard impenetrable wall placed at the origin. A schematic plot of the setup is shown in fig. 1 for $N = 5$ particles represented as Gaussian wave packets. For positive times, t , the particles are allowed to explore the positive real line. The quantum state of

the system is described by the N -particle wave function $\Psi(x_1, \dots, x_N, t)$, which satisfies the time-dependent Schrödinger equation,

$$i \frac{\partial}{\partial t} \Psi(x_1, \dots, x_N, t) = \hat{H}^{(N)} \Psi(x_1, \dots, x_N, t), \quad (1)$$

where $\hat{H}^{(N)} = -\frac{1}{2} \left(\frac{\partial^2}{\partial x_1^2} + \dots + \frac{\partial^2}{\partial x_N^2} \right)$ is the N -particle Hamiltonian operator and we have set the Planck's constant and particle masses to unity. The initial wave function is such that $\Psi(x_1, \dots, x_N, t=0) = 0$ if $x_j \neq I$ for all $j \in [1, N]$.

Under time evolution, the wave function diffuses outside I . One way to measure this is through the survival probability $P^{(N)}(t)$, *i.e.*, the probability that all N quantum particles are in I at times $t > 0$. In terms of the wave function, the survival probability is defined as

$$P^{(N)}(t) = \int_{I^N} |\Psi(x_1, \dots, x_N, t)|^2 dx_1 \dots dx_N. \quad (2)$$

Quantum statistics obeyed by the N particles—whether bosonic or fermionic—can have a dramatic effect on the time decay of the survival probability. More specifically, it was observed in ref. [3] that the survival probability $P^{(2)}(t)$ asymptotically decays to zero as $\sim t^{-6}$ for bosons and $\sim t^{-10}$ for fermions; a surprisingly simple, yet generic, result obtained by an asymptotic expansion of the appropriate quantum propagator for large t . This

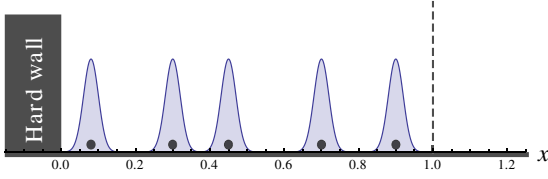


Fig. 1: (Color online) Schematic plot of the initial configuration for $N = 5$ particles represented as Gaussian wave packets.

was later generalized in ref. [5] for N particles, showing that $P^{(N)}(t)$ decays like $\sim t^{-3N}$ and $\sim t^{-N(2N+1)}$ for bosons and fermions, respectively. The faster fermionic decay was attributed to the effective hard-core interaction among fermions causing anti-bunching and hindering the reconstruction of the initial state. In both works [3,5] Dirichlet boundary conditions were imposed at the hard wall.

When a particle is constrained to move within a limited volume, Dirichlet (\mathcal{D}) or Neumann (\mathcal{N}) boundary conditions (BCs) are usually employed in order to reflect local probability preservation at $x=0$. It is well known, however, that the general solution to this requirement is described by a Robin (\mathcal{R}) BC [12], defined as a weighted combination of the \mathcal{D} and \mathcal{N} BCs

$$\left(\frac{\partial}{\partial x_j} - \eta\right) \Psi(x_1, \dots, x_N, t) \Big|_{x_j=0} = 0, \quad \forall j, \quad (3)$$

and controlled by the parameter $\eta \in \mathbb{R}$, such that $\eta=0$ corresponds to the \mathcal{N} and $\eta=\infty$ to the \mathcal{D} BCs. The parameter η has the physical interpretation of a phase shift on reflection with the wall. Therefore, the following natural question arises: *What is the influence of boundary conditions on the decay of the survival probability?* More specifically, *how does the survival probability $P^{(N)}(t)$ depend on η ?* This we address in the current setting by deriving and analyzing the exact quantum propagator.

While of clear mathematical interest, such generalized BCs have important practical applications and are commonly used in Sturm-Liouville-type problems when modeling acoustic and convection-diffusion processes. In quantum mechanics, \mathcal{R} BCs are relevant in, *inter alia*, surface effects within the Ginzburg-Landau theory of normal-superconducting interfaces [13], wetting theory [14] and electronic transport through waveguides and nano-wires [15]. Significantly, the additional freedom provided by η is similar to the variation of any external parameter in a Hamiltonian system and can for example prove a powerful tool in the spectral analysis of quantum billiards [16].

We now motivate our investigation by considering the simplest case of escape from I involving just a single particle. The dynamical evolution of the wave function can be described by the quantum propagator $K_\eta(x, x', t)$ as

$$\Psi(x, t) = \int_I K_\eta(x, x', t) \Psi(x', 0) dx'. \quad (4)$$

The propagator [17] is a generalized function that satisfies the time-dependent Schrödinger equation

$$\left(i\frac{\partial}{\partial t} + \frac{1}{2}\frac{\partial^2}{\partial x^2}\right) K_\eta(x, x', t) = 0, \quad (5)$$

the initial condition $\lim_{t \rightarrow 0} K_\eta(x, x', t) = \delta(x - x')$ and the \mathcal{R} BC at $x=0$

$$\left(\frac{\partial}{\partial x} - \eta\right) K_\eta(x, x', t) \Big|_{x=0} = 0, \quad (6)$$

and that vanishes as $x \rightarrow \infty$ at negative imaginary times, *i.e.* $\lim_{x \rightarrow \infty} K_\eta(x, x', -iT) = 0$ for $T > 0$.

The cases of $\eta=0$ (\mathcal{N} BC) and $\eta=\infty$ (\mathcal{D} BC) are particularly simple. Using the method of images we can immediately write down the full single-particle propagator

$$K_0(x, x', t) = K_{\text{free}}(x, x', t) + K_{\text{free}}(x, -x', t), \quad (7)$$

$$K_\infty(x, x', t) = K_{\text{free}}(x, x', t) - K_{\text{free}}(x, -x', t), \quad (8)$$

where

$$K_{\text{free}}(x, x', t) = \frac{1}{\sqrt{2\pi it}} \exp\left(-\frac{(x-x')^2}{2it}\right), \quad (9)$$

is the free-particle propagator describing the motion on the real line without a reflecting wall at the origin.

The asymptotic decay of $P^{(1)}(t)$ is entirely determined by the long-time expansion of the propagator. Thus, $K_0(x, x', t) = \sqrt{\frac{2}{i\pi t}} + \mathcal{O}(t^{-3/2})$ and $K_\infty(x, x', t) = -\sqrt{\frac{2i}{\pi}} \frac{xx'}{t^{3/2}} + \mathcal{O}(t^{-5/2})$, entailing that $P^{(1)}$ decays like $\sim t^{-1}$ for \mathcal{N} BC and $\sim t^{-3}$ for \mathcal{D} BC. For alternative analytic approaches using Moshinsky functions see ref. [2].

When addressing the case of two particles, the issue of quantum statistics comes into play. For non-interacting particles, there are two ways of taking into account bosonic (b) or fermionic (f) statistics: either i) by appropriately symmetrizing the initial state of the system,

$$\Psi^{(b/f)}(x_1, x_2, 0) = \frac{1}{\sqrt{2}} [\psi_1(x_1)\psi_2(x_2) \pm \psi_1(x_2)\psi_2(x_1)], \quad (10)$$

with “+” corresponding to bosons and “−” to fermions, and propagating it with $K_\eta(x_1, x'_1, t)K_\eta(x_2, x'_2, t)$, or ii) by introducing an effective, appropriately symmetrized two-particle propagator

$$K_\eta^{(b/f)}(x_1, x_2, x'_1, x'_2, t) = \frac{1}{\sqrt{2}} \left[K_\eta(x_1, x'_1, t)K_\eta(x_2, x'_2, t) \pm K_\eta(x_2, x'_1, t)K_\eta(x_1, x'_2, t) \right] \quad (11)$$

and applying it upon the product state $\psi_1(x_1)\psi_2(x_2)$. Indeed, the two-particle state at $t > 0$ can be written as

$$\begin{aligned} \Psi^{(b/f)}(x_1, x_2, t) = & \int_{I^2} K_\eta(x_1, x'_1, t)K_\eta(x_2, x'_2, t) \Psi^{(b/f)}(x'_1, x'_2, 0) dx'_1 dx'_2 = \\ & \int_{I^2} K_\eta^{(b/f)}(x_1, x_2, x'_1, x'_2, t) \psi_1(x'_1)\psi_2(x'_2) dx'_1 dx'_2, \quad (12) \end{aligned}$$

where the first equality corresponds to case i) and the second to case ii). Being interested in the asymptotics of the survival probability we adopt approach ii), as it allows us to focus only on the kernel, as opposed to the full integral. In other words, the long-time decay of $P^{(2)}(t)$ is determined by $K_\eta^{(b/f)}$ in the limit $t \rightarrow \infty$. One obtains that $K_0^{(b)} \sim t^{-1}$, $K_0^{(f)} \sim t^{-3}$, $K_\infty^{(b)} \sim t^{-3}$ and $K_\infty^{(f)} \sim t^{-5}$. The asymptotic behavior of $P^{(2)}(t)$ is simply the square of $K_\eta^{(b/f)}$. It is interesting to note that the asymptotic decay of the survival probability of two fermions with the \mathcal{N} BC is governed by the same exponent as that of two bosons with the \mathcal{D} BC. This simple observation clearly illustrates that BCs imposed at the perfectly reflecting wall are as important for the particle escape as quantum statistics. It also suggests that by tuning the value of η one may expect to probe the continuum of possible decay rates, ranging between those for the \mathcal{D} and \mathcal{N} BCs. However, as we shall show this is not the case, and the decay exponent turns out to be a discontinuous function of η .

Single-particle case. – Unlike in the special cases of $\eta = 0$ (\mathcal{N} BC) and $\eta = \infty$ (\mathcal{D} BC), the quantum propagator for an arbitrary η can not be straightforwardly obtained using the method of images; alternative techniques have to be employed. We begin our study of the single-particle survival probability by deriving an exact closed-form expression for K_η defined through eqs. (5), (6).

Exact propagator. One way to construct the single-particle propagator $K_\eta(x, x', t)$ is by using a complete orthonormal set of eigenstates $\{\phi_k\}$ of the Hamiltonian $\hat{H}^{(1)}$,

$$-\frac{1}{2} \frac{d^2}{dx^2} \phi_k(x) = E_k \phi_k(x), \quad (13)$$

satisfying the \mathcal{R} BC at the origin, $(\frac{d}{dx} - \eta) \phi_k(0) = 0$. As will become clear from the following discussion (and as originally noted in ref. [18] within the context of identical quantum particles), there is an important spectral difference between the case of $\eta > 0$ and that of $\eta < 0$. We analyze the two cases in succession.

In the case of $\eta > 0$, the energy spectrum of $\hat{H}^{(1)}$ is continuous. Indeed, the corresponding eigensystem is

$$\phi_k(x) = \sqrt{\frac{2}{\pi \left(1 + \frac{k^2}{\eta^2}\right)}} \left[\sin(kx) + \frac{k}{\eta} \cos(kx) \right] \quad (14)$$

with $E_k = k^2/2$ and $k > 0$. The Hamiltonian eigenstates for the \mathcal{N} and \mathcal{D} BCs are, respectively, obtained as the limits $\lim_{\eta \rightarrow 0} \phi_k(x) = \sqrt{\frac{2}{\pi}} \cos(kx)$ and $\lim_{\eta \rightarrow \infty} \phi_k(x) = \sqrt{\frac{2}{\pi}} \sin(kx)$.

It can be verified by direct integration that the set of the eigenstates $\{\phi_k\}$ is orthonormal: $\int_0^\infty \phi_k(x) \phi_{k'}(x) dx = \delta(k - k')$, and complete: $\int_0^\infty \phi_k(x) \phi_k(x') dk = \delta(x - x')$.

Consequently, the propagator expressed in the basis formed by $\{\phi_k\}$, reads

$$K_\eta(x, x', t) = \langle x | e^{-i\hat{H}^{(1)}t} | x' \rangle = \int_0^\infty \phi_k(x) \phi_k(x') e^{-i\frac{k^2}{2}t} dk. \quad (15)$$

Using (14), the integral in eq. (15) can be rewritten as

$$\begin{aligned} \mathcal{I}_1 - \mathcal{I}_2 &= \frac{1}{2\pi} \int_{-\infty}^{+\infty} [\cos(x_+k) + \cos(x_-k)] e^{-\frac{1}{2}ik^2t} dk \\ &\quad - \frac{\eta}{\pi} \int_{-\infty}^{+\infty} \frac{\eta \cos(x_+k) - k \sin(x_+k)}{k^2 + \eta^2} e^{-\frac{1}{2}ik^2t} dk \end{aligned} \quad (16)$$

with $x_\pm = x \pm x'$. Then, it is easy to see that the first term is nothing but the quantum propagator for the \mathcal{N} BC, *i.e.* $\mathcal{I}_1 = K_0(x, x', t)$. The second term yields $\mathcal{I}_2 = \eta \operatorname{erfc}\left(\frac{x_+ + i\eta t}{\sqrt{2it}}\right) e^{\eta x_+ + \frac{1}{2}i\eta^2 t}$, where “erfc” denotes the complementary error function. Combining the two terms we obtain our first main result

$$K_\eta(x, x', t) = K_0(x, x', t) - \eta \operatorname{erfc}\left[\frac{x + x' + i\eta t}{\sqrt{2it}}\right] e^{\eta(x+x') + \frac{1}{2}i\eta^2 t}. \quad (17)$$

In the case of $\eta < 0$, the set of eigenstates $\{\phi_k\}$ no longer forms a complete basis [18]. Indeed, in addition to the unbound eigenstates, forming a continuous part of the energy spectrum, there exists an isolated bound state

$$\chi(x) = \sqrt{2|\eta|} e^{-|\eta|x}, \quad \eta < 0, \quad (18)$$

with negative energy $-\eta^2/2$, *i.e.* $\hat{H}^{(1)}|\chi\rangle = -\frac{\eta^2}{2}|\chi\rangle$. The state is normalized to unity, $\langle \chi | \chi \rangle = 1$, and is orthogonal to the eigenstates of the continuous part of the energy spectrum, *i.e.* $\langle \chi | \phi_k \rangle = 0$ for any k . The wave function $\chi(x)$ is localized in the vicinity of the hard wall, indicating that the BCs here correspond to an effective zero-range attractive force. Bound states in one-dimensional escape problems have also been discussed in ref. [2]. There, however, the bound state is intrinsic to the shape of the trapping potential and not the BCs used.

The bound state modifies the completeness relation to

$$\int_0^\infty \phi_k(x) \phi_k(x') dk + \chi(x) \chi(x') = \delta(x - x'), \quad \eta < 0, \quad (19)$$

so that the propagator expanded in terms of the complete basis $(\{\phi_k\}, \chi)$ reads (cf. eq. (15))

$$K_\eta(x, x', t) = \int_0^\infty \phi_k(x) \phi_k(x') e^{-\frac{1}{2}ik^2t} dk + \chi(x) \chi(x') e^{i\frac{\eta^2}{2}t}. \quad (20)$$

The evaluation of the last integral for $\eta < 0$ proceeds in the same manner as in the case of $\eta > 0$, and the resulting expression for the full propagator coincides with that given

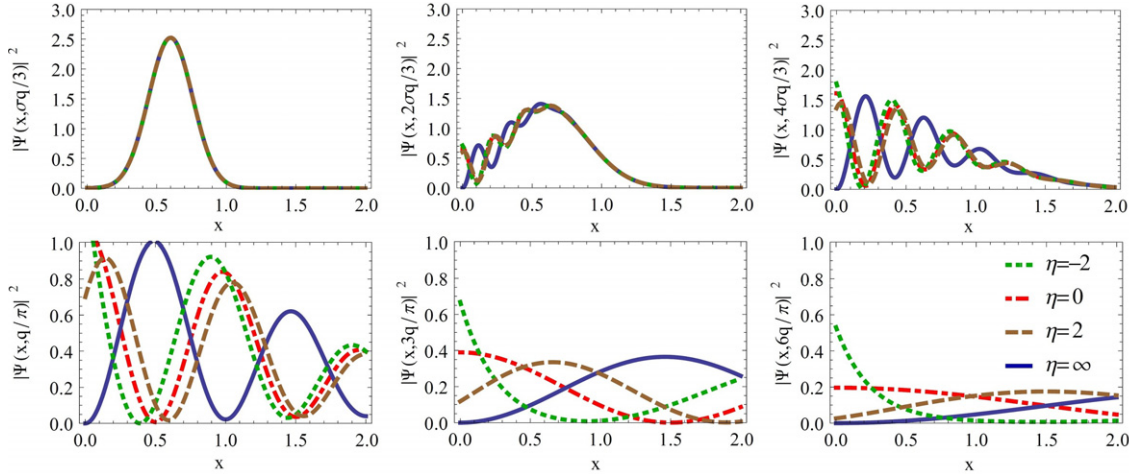


Fig. 2: (Color online) Snapshots of the evolution of the density $|\Psi(x,t)|^2$ of a Gaussian wave packet initially centered at $q=0.6$ with width $\sigma=0.1$ at times $t=t_w, 2t_w, 4t_w$ (top panels) and at $t=t_a, 3t_a, 6t_a$ (bottom panels). The values $t_w = q\sigma/3$ and $t_a = q/\pi$ are, respectively, the approximate times when the wave packets start interacting with the wall, and when the asymptotic regime sets in (see the discussion in the main text for details). The four curves in each panel correspond to the evolution under different propagators K_η with $\eta = \infty, 0, 2$, and -2 as indicated in the last panel.

by eq. (17). This concludes our derivation of the single-particle propagator.

At this point we remark that the problem of a single particle restricted to the positive real line by a hard wall, is equivalent to that of two hard-core particles on the full real line through a change of variables to center of mass and relative coordinates. Moreover, the BCs imposed in the former correspond to the quantum statistics obeyed by the latter allowing for the possibility of anyons [18]. The equivalence in the case of many particles is however more subtle with essential differences in higher dimensions.

Short-time dynamics. Knowledge of the exact propagator (17) allows us to study the full dynamical evolution of the single-particle wave function $\Psi(x,t)$. In particular, in order to understand the influence of BCs on the escape, it is instructive to apply K_η to a spatially localized initial state given by a Gaussian wave packet $\Psi(x,0) = (\pi\sigma^2)^{-1/4} \exp(-\frac{(x-q)^2}{2\sigma^2})$, centered at $q \in (3\sigma, 1-3\sigma)$ with spatial width $\sigma \ll 1$, such that $\Psi(x \notin I, 0) \approx 0$.

Figure 2 shows snapshots at different times of the probability density function $|\Psi(x,t)|^2$ under time evolution by K_η for four different values of η . We denote these four cases by: i) $\eta = \infty$, ii) $\eta = 0$, iii) $\eta = 2$ and iv) $\eta = -2$. For the first two simple cases i) and ii) (corresponding to the blue and red curves in fig. 2), the density can be written down explicitly as

$$|\Psi(x,t)|^2 = \frac{2}{\sigma\sqrt{\pi}} \frac{e^{-\frac{\theta^2}{1+\tau^2}}}{\sqrt{1+\tau^2}} e^{-\frac{\xi^2}{1+\tau^2}} \times \left[\cosh\left(\frac{2\xi\theta}{1+\tau^2}\right) \mp \cos\left(\frac{2\tau\xi\theta}{1+\tau^2}\right) \right], \quad (21)$$

where we have used the scaled variables $\tau = t/\sigma^2 > 0$, $\xi = x/\sigma$, and $\theta = q/\sigma$, for the sake of brevity. The “ $-$ ”

and “ $+$ ” signs in (21) correspond to cases i) and ii), respectively. Cases iii) and iv) in the figure were calculated through numerical integration of eq. (4). Inspecting eq. (21) we can identify the first exponential as the main time envelope and its denominator as being indicative of the diffusive process. The cosine term describes the oscillations due to interaction with the wall and are clearly seen in fig. 2.

We now qualitatively describe the dynamics observed in fig. 2 with the aid of eq. (21) and identify three distinctly different time scales. For times $0 < t \leq t_w$, all four curves coincide as they diffuse freely until the wave packets start interacting with the wall. This occurs when $3\sigma\sqrt{1-\tau^2} \approx q$, and so $t_w \approx q\sigma/3$ for $\sigma \ll 1$. For times $t > t_w$, oscillations appear due to reflection off the wall and interference occurs. The wall interaction, however, is different in each case due to the different BCs prescribed by η . It is clear from the figure that i) and ii) are completely out of phase, while iii) and iv) closely follow curve ii) and are only slightly out of phase. The oscillations spread until $t \approx t_a$, when there is only a single maximum of $|\Psi(x,t)|^2$ left in I for case i) and a single minimum for case ii). The time t_a can be extracted from the cosine term in eq. (21) by requiring its argument to be 2π at $x=1$. We thus have that $t_a \approx q/\pi$ for $\sigma \ll 1$. Indeed, at times greater than t_a , the asymptotic regime sets in and there are no more oscillations. Cases i) to iii) behave essentially the same, as they diffuse at different rates while case iv) seems to “stick” to the wall. The difference between iii) and iv) can be clearly seen in the GIF animations included as supplementary material¹.

¹Two GIF animations (PSIeta+.gif and PSIeta-.gif) showing a Gaussian wave packet diffusing with time to the right while being reflected off a hard wall at zero with Robin boundary conditions and control parameters $\eta = 2$ and -2 .

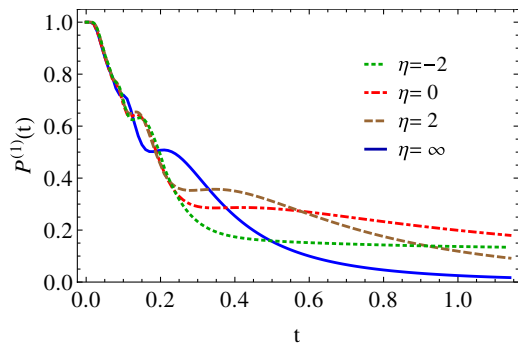


Fig. 3: (Color online) The single-particle survival probability for the four cases described in fig. 2 using the same values for q and σ . The asymptotic regime sets in around $t_a = q/\pi \approx 0.191$.

Figure 3 shows the survival probability (2) for the four cases considered above for times up to $6t_a$, with the same parameters used in fig. 2. Cases i) and ii) were calculated analytically, while iii) and iv) by numerically integrating eqs. (4) and (2). An additional time scale to the three described above now becomes relevant. For times $t \leq t_d$ the Gaussian wave packets have not spread outside I and so there is not decay and $P^{(1)}(t \leq t_d) = 1$. Hence we have that $t_d = (1 - q)/3\sigma$. Note that t_d can be smaller, larger or equal to t_w , depending on the value of q . From fig. 3 we notice that $P^{(1)}(t)$ is decreasing non-monotonically and shows strong oscillations. These are due to the spreading of the interference oscillations observed in fig. 2. Moreover, there are a finite number of oscillations as for $t \gg 1$, the frequency in the cosine term of eq. (21) goes to zero. We can estimate the number of oscillations by $\int_{t_w}^{t_a} \frac{q}{\pi t^2} dt = \frac{3}{\pi\sigma} - 1$ for $\sigma \ll 1$.

For times $t \gg \sigma^2$, the two exponentials and the hyperbolic cosine of eq. (21) are approximately equal to 1. Using this approximation and integrating over $x \in I$ we obtain an approximation for $P^{(1)}(t)$ for cases i) and ii)

$$P^{(1)}(t) \approx \frac{2\sigma}{\sqrt{\pi}t} \left[1 \mp \frac{\sigma}{2q} \sin\left(\frac{2q}{t}\right) \right]. \quad (22)$$

Expanding for large times produces the expected asymptotics. Note that for case i), the order t^{-1} term cancels exactly, so $P^{(1)}(t) \sim t^{-3}$.

Asymptotic analysis. In the limits $\eta \rightarrow 0$ and $\eta \rightarrow \infty$ we obtain the propagators with \mathcal{N} and \mathcal{D} BCs, respectively, as expected, with next-to-leading-order corrections:

$$K_\eta(x, x', t) = K_0(x, x', t) - \operatorname{erfc}\left[\frac{\sqrt{-i}(x+x')}{\sqrt{2t}}\right] \eta \quad (23)$$

and

$$K_\eta(x, x', t) = K_\infty(x, x', t) - \frac{2i(x+x')}{\eta t} K_{\text{free}}(x, -x', t). \quad (24)$$

In the limit of $\eta \rightarrow -\infty$, however, we obtain

$$K_\eta(x, x', t) = -2|\eta|e^{-|\eta|(x+x') + \frac{1}{2}it\eta^2} + K_\infty(x, x', t), \quad (25)$$

which implies that for negative (but finite) values of η , the single-particle survival probability saturates at some constant, rather than decaying to zero, as observed in fig. 3. In the limit this constant vanishes and $K_\infty = K_{-\infty}$.

To understand this better we expand eq. (17) for large times t to get

$$K_\eta(x, x', t) = (|\eta| - \eta)e^{\eta(x+x') + \frac{1}{2}it\eta^2} - \frac{(1+i)(1+x\eta)(1+x'\eta)}{\sqrt{\pi}\eta^2 t^{3/2}} + \mathcal{O}(t^{-5/2}). \quad (26)$$

Note that the first term vanishes when $\eta \geq 0$. Equation (26) confirms that for $\eta > 0$ the asymptotic single-particle survival probability decays like $\sim t^{-3}$ (as for \mathcal{D} BC) and for $\eta < 0$ the decay saturates at a constant \mathcal{C} . Applying the first term in (26) to a Gaussian initial state

$$\mathcal{C} = 4|\eta|\sigma e^{-2q|\eta|}(1 - e^{-2|\eta|}) + \mathcal{O}(\sigma^2) \approx 4|\eta|\sigma e^{-2q|\eta|}, \quad (27)$$

indicating that the \mathcal{C} is maximal approximately when $\eta = -1/(2q)$. Hence, the decay properties of the survival probability can depend strongly on the initial state chosen. For instance if the initial state is orthogonal to the bound state $\chi(x)$ then $\mathcal{C} = 0$.

We remark that eq. (26) can be seemingly misleading, since for $\eta = 0$ (corresponding to \mathcal{N} BC) the second term diverges like $\sim -\sqrt{2i}/(\sqrt{\pi}\eta^2 t^{3/2})$. Indeed this implies that the limit $\eta \rightarrow 0$ does not commute with that of $t \rightarrow \infty$. In fact we notice that eq. (26) reproduces the correct asymptotics, only if η scales like $\sqrt{1/t}$. This can be understood in the following way: for $\eta < 0$, the bound state χ becomes completely delocalized in the limit $\eta \rightarrow 0^-$. One can then imagine that χ acts like an “ η -thin carpet” hindering the particle diffusion, thus giving a slower decay of $P^{(1)} \sim t^{-1}$.

In brief, the exponent α of the asymptotic power law decay $P^{(1)} \sim t^{-\alpha}$ experiences discontinuous jumps from 0 for $\eta < 0$, to 1 for $\eta = 0$, and 3 for $\eta > 0$. This unexpected discontinuity has interesting repercussions when considering the escape of $N \geq 2$ particles from the interval $I = (0, 1)$ and are discussed in the next section. Note that α can also vary depending on the initial state [19].

Many-particle case. – In the case of two particles, the initial state is given by eq. (10) with $\psi_j(x) = (\pi\sigma_j^2)^{-1/4} \exp\left(-\frac{(x-q_j)^2}{2\sigma_j^2}\right)$, for $j = 1, 2$, and the wave function $\Psi^{(b/f)}(x_1, x_2, t)$ at a later time $t > 0$ is determined by eqs. (11) and (12). We have previously discussed the asymptotic behavior of $P^{(2)}$ for \mathcal{N} and \mathcal{D} BCs and now turn to the general case of arbitrary η . This is achieved by expanding the propagator (11) in the limit of large t as seen in table 1. It is interesting to note that the anti-symmetry of the fermionic wave function does not allow for

Table 1: The asymptotic survival probability for one, two, and N particles, as well as different BCs.

\mathcal{R} BC	1	2 bos	2 fer	N bos	N fer
$\eta < 0$	const	const	t^{-3}	const	$t^{(1-N)(2N-1)}$
$\eta = 0$	t^{-1}	t^{-2}	t^{-6}	t^{-N}	$t^{-N(2N-1)}$
$\eta > 0$	t^{-3}	t^{-6}	t^{-10}	t^{-3N}	$t^{-N(2N+1)}$
$\eta = \pm\infty$	t^{-3}	t^{-6}	t^{-10}	t^{-3N}	$t^{-N(2N+1)}$

a bound state and thus $P^{(2)}$ decays to zero. This completes the picture for the two-particle case.

The propagator (11) can be generalized for $N \geq 2$ particles in a standard way [20]:

$$K_{\eta}^{(b/f)}(x_1, \dots, x_N, x'_1, \dots, x'_N, t) = \frac{1}{\sqrt{N!}} \sum_{i_1, \dots, i_N=1}^N \varepsilon_{i_1, \dots, i_N} K_{\eta}(x_1, x'_{i_1}, t) \dots K_{\eta}(x_N, x'_{i_N}, t), \quad (28)$$

where $\varepsilon_{i_1, \dots, i_N}$ is the totally anti-symmetric (permutation) symbol in the case of fermions and identically 1 for bosons.

As done before, the asymptotic decay is obtained by expanding eq. (28) for large times t . We present the results for $N = 1, 2$, and for the general case in table 1 allowing for a direct comparison. In particular, we observe that the case of $\eta > 0$ coincides with that of $\eta = \pm\infty$. For the case of $\eta < 0$, the probability decays to a constant for bosons due to the presence of a bound state. Significantly, we observe that the case of $\eta = 0$ (\mathcal{N} BC) is special as it separates the other cases in a discontinuous fashion for both bosons and fermions. We also observe that fermions always escape faster than bosons. As we have previously pointed out, the asymptotic decay for two fermions with \mathcal{N} BC is the same as for two bosons with \mathcal{D} BC. However, this correspondence no longer holds for $N > 2$. Finally, we note that the survival probability of N fermions with $\eta > 0$ (or $\eta = \pm\infty$) has the same decay exponent as that of $N - 1$ fermions with $\eta < 0$.

Conclusions. – We have addressed the influence of boundary conditions on the escape of N indistinguishable particles in a one-dimensional setting, and we have shown that they are equally important as the prescribed quantum statistics. To this end, we have treated the problem in full detail and we have derived an exact closed form expression for the single-particle propagator on the positive real line in the presence of Robin boundary conditions with a single control parameter η . This expression generalized existing results and unveiled new non-trivial scenarios where escape may be suppressed. Moreover, we have found that the exponent of the asymptotic power law decay

of the survival probability is a discontinuous function of η . Our results hold for an arbitrary number of identical particles and are summarized in table 1.

In the light of recent atom-optics experiments addressing the dynamics of a small number of bosons and fermions in one dimension [11], our findings may lead to new applications in the area of quantum control and state manipulation. On the theoretical side, it is also interesting to explore how higher-dimensional waveguide-like [21] or network geometries [22], external potentials, particle-particle interactions may affect the dynamics and in particular quantum escape.

The authors thank CHRIS JOYNER and SUSUMU SHINOHARA for helpful discussions. GG acknowledges support from the Ministry of Science, Serbia (Project III 45010).

REFERENCES

- [1] ALTMANN E. G. *et al.*, to be published in *Rev. Mod. Phys.* (2012).
- [2] VAN DIJK W. and NOGAMI Y., *Phys. Rev. C*, **65** (2002) 024608.
- [3] TANIGUCHI T. and SAWADA S., *Phys. Rev. E*, **83** (2011) 026208.
- [4] TANIGUCHI T. and SAWADA S., *Phys. Rev. A*, **84** (2011) 062707.
- [5] DEL CAMPO A., *Phys. Rev. A*, **84** (2011) 012113.
- [6] GARCÍA-CALDERÓN G. and MENDOZA-LUNA L. G., *Phys. Rev. A*, **84** (2011) 032106.
- [7] PONS M. *et al.*, *Phys. Rev. A*, **85** (2012) 022107.
- [8] HAHN W. and FINE B. V., *Phys. Rev. A*, **85** (2012) 032713.
- [9] WALTNER D. *et al.*, *Phys. Rev. Lett.*, **101** (2008) 174101.
- [10] SERWANE F. *et al.*, *Science*, **332** (2011) 336.
- [11] ZÓRN G. *et al.*, *Phys. Rev. Lett.*, **108** (2012) 075303.
- [12] GUSTAFSON K. and ABE T., *Math. Intelligencer*, **20** (1998) 63.
- [13] DE GENNES P. G., *Superconductivity of Metals and Alloys* (Addison-Wesley) 1989.
- [14] BURKHARDT T. W., *Phys. Rev. B*, **40** (1989) 6987.
- [15] OLENSKI O. and MIKHAILOVSKA L., *Phys. Rev. E*, **81** (2010) 036606.
- [16] SIEBER M. *et al.*, *J. Phys. A: Math. Gen.*, **28** (1995) 5041.
- [17] BARTON G., *Elements of Green's Functions and Propagation* (Oxford Science Publications) 1989.
- [18] LEINAAS J. and MYRHEIM J., *Nuovo Cimento B*, **37** (1977) 1.
- [19] MIYAMOTO M., *Phys. Rev. A*, **68** (2003) 022702.
- [20] MESSIAH A., *Quantum Mechanics* (Dover Publications) 1999.
- [21] MATTHEWS J. C. F. and THOMPSON M. G., *Nature*, **484** (2012) 47.
- [22] COON J., DETTMANN C. P. and GEORGIU O., *Phys. Rev E*, **85** (2012) 011138.